4D Flow Characteristics After Aortic Valve Neocuspidization in Pediatric Patients: a Comparison with the Ross Procedure

Paolo Ciancarella[1]; Elena Milano[2,3]; Matteo Trezzi[4]; Claudio Capelli[2]; Paolo Ciliberti[4]; Enrico Cetrano[4]; Davide Curione[1]; Teresa Pia Santangelo[1]; Carmela Napolitano[1]; Veronica Bordonaro[1]; Sonia B. Albanese[4]; Adriano Carotti[4]; Aurelio Secinaro[1]

[1]Department of Imaging, Advanced Cardiovascular Imaging Unit, Bambino Gesù Children's Hospital, IRCCS, Rome, Italy
[2]University College London, Institute of Cardiovascular Science, and Great Ormond Street Hospital for Children, London, United Kingdom
[3]Department of Surgery, Paediatrics and Obstetrics, University of Verona, Verona, Italy
[4]Department of Pediatric Cardiology and Cardiac Surgery, Bambino Gesù Children's Hospital, IRCCS, Rome, Italy

Introduction

The optimal management of aortic valve (AV) disease in children is still challenging. If AV replacement (AVR) is indicated, four main types of AV substitutes are generally considered: pulmonary autografts (i.e., the Ross procedure), mechanical valves, biological valve prostheses, or homografts [1]. Although each option has specific advantages and drawbacks [2], the Ross procedure, first reported in 1967 [3], currently represents the preferred choice in children[1] with severe AV dysfunction [4, 5]. However, concerns regarding autograft dilatation and durability of both autograft and pulmonary conduit are far from negligible, suggesting a growing need for development of alternative solutions [6]. In this context, there is a rising interest in AV neocuspidization (AV Neo) using the technique described by Ozaki [7], which showed satisfactory freedom from reoperation at follow-up in an adult population [8]. The use of the Ozaki technique in children, as an alternative to the Ross procedure, has shown promising results, but it is burdened by limited follow-up and hemodynamic profile data [9, 10].

Aortic blood flow visualization and quantification throughout the cardiac cycle have recently been studied by 4D flow cardiovascular magnetic resonance imaging (CMR) in both congenital and acquired heart disease, such as bicuspid AV (BAV) [11], ascending aorta (AAo) dilatation [12], and aortic coarctation [13]. Specifically, in AV disease, asymmetrical leaflet opening causes abnormal rotational flow that hits the aortic wall [14] and is associated with increased wall shear stress and AAo diameters [11, 12].

In Ross patients, 4D flow CMR studies showed a laminar flow pattern in the AAo [15], comparable to a physiological hemodynamic profile. On the other hand, there is no data in the literature regarding AV Neo patients.

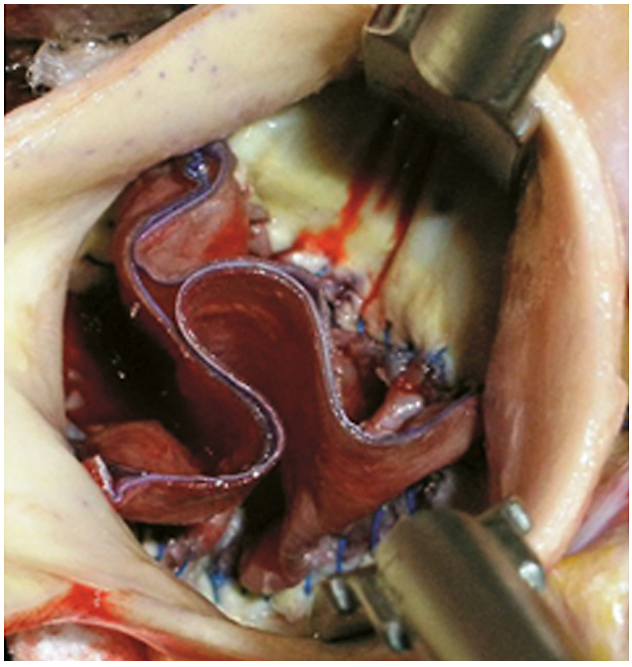

1 **Aortic valve reconstruction with Ozaki procedure**
The neo-cusps were reconstructed and then sutured to the annulus with the creation of three commissures, in line with the Ozaki neocuspidization technique.

[1]*MR scanning has not been established as safe for imaging fetuses and infants younger than two years of age. The responsible physician must evaluate the benefits of the MR examination compared to those of other imaging procedures.*

We therefore aimed to study a population of patients undergoing either Ross or AV Neo surgery at our institution to compare the hemodynamic profile following the two procedures. The study was conducted using 4D flow CMR and the hemodynamic assessment included both aortic root and AAo analysis in all patients.

Methods

Study population

Twenty patients who underwent AV replacement at our institution were prospectively recruited for this study. The study population included a group of ten consecutive patients who underwent AV Neo (AV Neo group) and a group of ten Ross patients (Ross group), enrolled for a follow-up CMR study.

The study complied with the Declaration of Helsinki and was approved by the local ethics committee; written informed consent was obtained for all participants.

Surgical procedures

The Ross procedure was mainly performed in patients with AV stenosis, while the AV Neo procedure was performed regardless of the preponderant anatomic lesion. The Ross procedure was carried out by autograft transplantation of the native pulmonary root using a standard full root technique, with coronary reimplantation and allograft reconstruction of the right ventricular outflow tract.

The details of the surgical technique used for AV Neo have been previously reported [16]; briefly, the aortic cusps were independently reconstructed with pericardium and sutured to the aortic annulus, with the creation of three new commissures (Fig. 1). The rationale of this technique is to preserve the anatomy of the aortic root and the physiological response throughout the whole cardiac cycle, including the coordination between aortic valve, annulus, left ventricle, sinus of Valsalva, and aorta. Moreover, by creating a large cooptation area with the reconstructed pericardial leaflets, it also ensures valve competence during annular growth and avoids lifelong anticoagulation therapy.

CMR acquisition protocol

All patients included in this study were prospectively recruited for follow-up CMR performed on a 1.5T scanner (MAGNETOM Aera, Siemens Healthcare, Erlangen, Germany) with an 18-channel body coil. Image acquisition settings and protocols were uniform throughout the study. The CMR protocol included conventional, retrospectively ECG-gated breath-hold balanced steady-state free precession (bSSFP) cine sequences. These were acquired in standard cardiac planes (long-axis views and short-axis stack) to quantify left ventricular volumes and function, and in dedicated AV and aortic root planes to evaluate leaflet excursion. Post-contrast ECG-gated 3D bSSFP magnetic resonance angiography (MRA) encompassing the whole thoracic aorta and triggered in mid-to-late diastole was obtained in the sagittal plane to measure aortic diameters.

A prototype 4D Flow gradient-echo sequence[2] (3D time-resolved phase-contrast imaging with three-directional velocity encoding) was acquired with retrospective ECG gating during free-breathing using a respiratory navigator placed at the lung-liver interface. The image acquisition volume was obtained in the sagittal plane encompassing the whole thoracic aorta. Technical parameters were as follows: isotropic voxel size ranging from 2.4 to 2.8 mm; field-of-view (FOV) read, 360–380 mm; FOV phase, 68.8–75%; matrix, 128 x 128 or 160 x 160; TR, 38 ms; TE, 2.3 ms; flip angle, 7°; receiver bandwidth, 496 Hz/pixel; parallel imaging (GRAPPA) along the phase encoding direction with a reduction factor R = 2 or 3. In order to optimize the velocity-to-noise ratio (VNR), the velocity encoding (VENC) range was determined using the lowest non-aliasing arterial velocity calculated on conventional 2D phase-contrast images. In our population, VENC values ranged between 180 and 400 cm/s depending on the presence and severity of valve acceleration. The sequence was acquired after intravenous contrast administration (gadoterate meglumine, DOTAREM, Roissy, Guerbet, France) at 0.2 mmol/kg, to improve image quality.

Image processing and analysis

Image processing and analysis was performed with a commercial software package (CMR42, Circle Cardiovascular Imaging Inc., Calgary, Canada). Left ventricular end-diastolic volume (LVEDV), end-systolic volume (LVESV), end-diastolic mass (LVEDM), and ejection fraction (LVEF) were calculated for each patient from short-axis cine bSSFP images. Papillary muscles and trabeculae were included in the blood pool. LVEDV, LVESV, and LVEDM were indexed for body surface area (BSA), calculated with the Mosteller formula.

Aortic measurements were obtained from 3D bSSFP MRA images; the diameter of the sinuses of Valsalva was the maximum value among the three sinus-to-sinus measurements, and the mid-AAo diameter was the maximum value between two orthogonal measurements in a cross-sectional plane at the level of pulmonary bifurcation. All the aortic measurements were taken from inner edge to inner edge of the vessel wall.

Pre-processing correction strategies were applied to all 4D Flow datasets in order to reduce phase offset errors and image noise. Moreover, data-quality evaluation was

[2] *Work in progress: the application is currently under development and is not for sale in the U.S. and in other countries. Its future availability cannot be ensured.*

performed to confirm measurement accuracy according to the literature [17], with quantitative comparison of 4D results and standard 2D phase-contrast sequences. 4D Flow datasets were processed to generate 3D interactive images of blood flowing through the thoracic aorta, visualized as Doppler-like color-coded streamlines and velocity vectors. After initial segmentation of the region of interest (from the left-ventricular outflow tract to the mid-descending aorta), the vessel centerline was automatically computed and manually adjusted when needed. Two reference planes perpendicular to the vessel centerline were identified at the sinotubular junction (P1) and at the point where the mid-AAo crosses the pulmonary bifurcation (P2). These landmarks were used to measure conventional flow and velocity parameters: forward flow (FF), backward flow (BF), net flow (NF), regurgitation fraction (RF), and maximum velocity (Vmax). The flow eccentricity index and wall shear stress were analyzed at the same levels. Blood flow eccentricity was evaluated on 2D color-coded velocity maps obtained in systole, and was semi-quantitatively graded by two operators (EM, PC) as central (grade 0), mildly eccentric (grade 1), or markedly eccentric (grade 2), in line with previous descriptions in the literature [18, 19] (Fig. 2). Wall shear stress (WSS, unit N/m^2) is a time-resolved 3D force obtained from 4D Flow datasets and calculated as axial, circumferential, and global components (Fig. 2). Both maximum and average WSS values were obtained.

Statistical analysis

Data analysis was performed using MedCalc ver. 15.8 (MedCalc Software Ltd., Ostend, Belgium). For statistical analysis, the Wilcoxon signed-rank test, the Mann-Whitney U test and the ANOVA test were used. A p value ≤ 0.05 was considered to be significant. Values are presented as mean ± standard deviation (SD) or as median and range, as appropriate.

Results

Aortic valvulopathy at the time of surgery was in most cases a congenital lesion, with BAV as the predominant diagnosis (65%). The baseline characteristics of patients are summarized in Table 1.

A data-quality check performed on phase-contrast datasets showed consistency of 4D Flow, with no significant discrepancies between 4D and 2D results. In addition, neither gross aliasing, nor aberrant streamlines/pathlines were visualized.

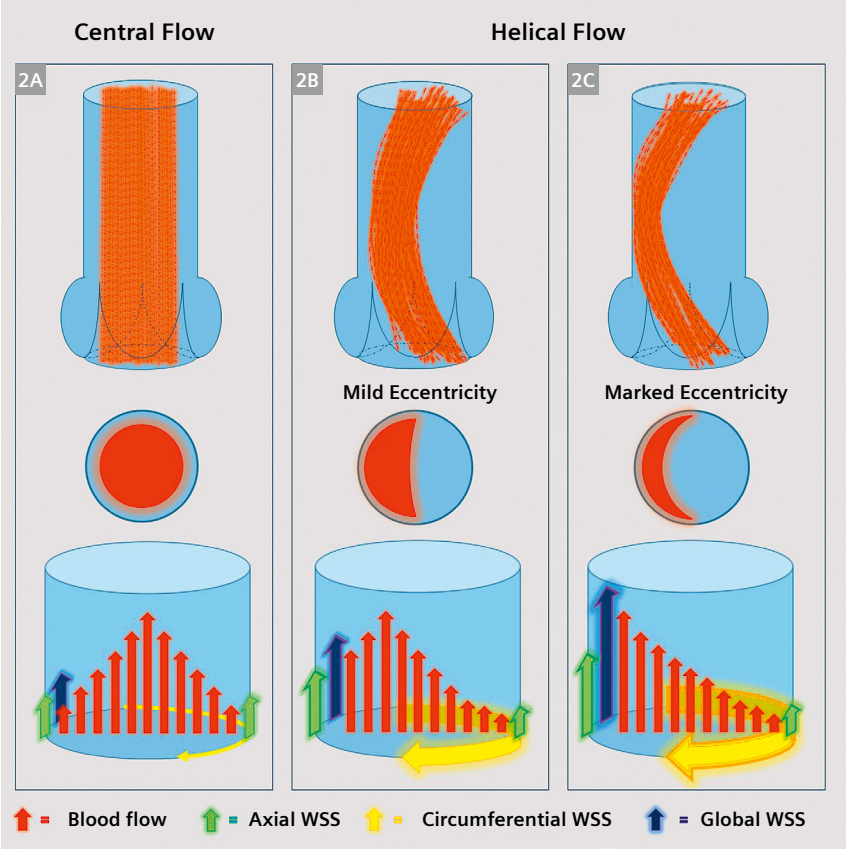

2 Wall shear stress in the ascending aorta
Different flow and wall shear stress patterns at the level of the ascending aorta: In central flow, high linear systolic flow is focused at the center and occupies the majority of the vessel lumen; axial WSS represents the main wall shear stress vector of global WSS (2A). In helical flow, the high systolic blood stream vectors are placed eccentrically toward the periphery of the vessel lumen and fill between one- and two-thirds of the vessel lumen (mild eccentricity, 2B) or one-third or less of the vessel lumen (marked eccentricity, 2C), with circumferential WSS representing the dominating vector of global WSS.

Ross procedure group

Median age at surgery was 10.6 years (range 3.9–16.5 years). Indications for the Ross procedure were aortic stenosis (n = 8), aortic regurgitation (n = 1), or mixed stenosis-regurgitation (n = 1). CMR imaging was performed at a median of 34 months after the operation (range 6–205 months). At follow-up, patients in the Ross group showed normal transvalvular max velocity (130 ± 33 cm/s) and peak gradient (7.0 ± 3.7 mmHg) across the aortic valve (Table 2), with mild regurgitation (RF 10.5 ± 12.7%).

AV Neo group

Median age at surgery was 11.4 years (range 7.1–15.9 years). Indications for the AV Neo procedure were aortic regurgitation (n = 5), aortic stenosis (n = 4), or mixed stenosis-regurgitation (n = 1).

CMR imaging was performed at a median of 4 months after the operation (range 1–10 months). At follow-up, patients in the AV Neo group showed slightly increased maximum velocity across the aortic valve (220 ± 73 cm/s) with no significant regurgitation (RF 9.3 ± 4.0%).

	Ross (n = 10)	AV Neo (n = 10)	p
Female (%)	1 (10%)	4 (40%)	0.12
Aortic valve defect (%)			
Bicuspid aortic valve	6 (60%)	7 (70%)	0.22
Aortic stenosis	8 (80%)	4 (40%)	0.07
Aortic regurgitation	1 (10%)	5 (50%)	0.05
Mixed stenosis/regurgitation	1 (10%)	1 (10%)	1
Age at surgery (years)	10.6 ± 4.2	11.4 ± 3.1	0.64
Age at scan (years)	16.2 ± 7.9	9.6 ± 2.9	*0.008
Surgery-to-scan time (months)	63.8 ± 64	4 ± 2.4	*0.0091
Body weight at scan (kg)	58.8 ± 17.8	47.5 ± 20.0	0.19
BSA at scan (m^2)	1.60 ± 0.33	1.36 ± 0.38	0.15
Aortic root indexed (mm/BSA)	24.2 ± 3.8	18.8 ± 5.6	*0.022
AAo indexed (mm/BSA)	17.0 ± 3.4	18.5 ± 5.0	0.45

Table 1: **Patient demographics**
Values expressed as average and standard deviation;
*statistically significant p values ($p < 0.05$)

	Ross (n = 10)	AV Neo (n = 10)	p
LVEDVi (ml/m^2)	91.2 ± 18.8	79.2 ± 14.4	0.12
LVESVi (ml/m^2)	37.6 ± 10.8	31.2 ± 13.4	0.19
LVEF (%)	59 ± 5	61.1 ± 7.2	0.46
CI ($L/min/m^2$)	3.47 ± 1.01	3.97 ± 1.04	0.29
LVEDMi (g/m^2)	64.7 ± 13.5	71.5 ± 11.1	0.23
Ao RF (%)	10.5 ± 12.7	9.3 ± 4.0	0.77
Ao Vmax (cm/sec)	130 ± 33	220 ± 73	*0.0024
Ao Gmax (mmHg)	7.1 ± 3.7	21 ± 13.8	*0.0065

Table 2: **Functional parameters**
Values expressed as average and standard deviation;
*statistically significant p values ($p < 0.05$).

Blood flow pattern and wall shear stress

Analysis of the flow pattern in patients who underwent either the Ross or the AV Neo procedure showed no clear association between an eccentric flow pattern and the operation performed (p = 0.058 at the sinotubular junction and p = 0.17 at the mid-AAo) (Figs. 3, 4).

At the sinotubular junction, Ross patients showed central flow in 40% of cases and mild eccentricity in 60% of cases, while AV Neo patients had central flow in 90% of cases and marked eccentricity in 10% of cases (inter-rater agreement Weighted K = 0.867). At the mid-AAo, Ross patients showed central flow in 30% of cases and mild eccentricity in 70% of cases, whereas AV Neo patients had central flow in 70% of cases, mild eccentricity in 20% of cases, and marked eccentricity in 10% of cases (inter-rater agreement Weighted K = 0.653). Figure 5 shows aortic fluid dynamics following AV Neo repair.

No significant differences between the two groups were observed in axial, circumferential, or global WSS measured at the sinotubular junction and at the mid-AAo (Table 3).

Discussion

In this study, we demonstrated that the Ross procedure and the AV Neo procedure show similar hemodynamic profiles, analyzed by 4D Flow CMR.

The influence of hemodynamic shear stress due to spatial and temporal alterations in shear forces on the endothelium has been described by others, showing regionally different flow and arterial remodeling [20]. The mechanical shear forces induced by blood flow seem to play an important role in the process of valve leaflet injury and vascular remodeling.

4D Flow CMR has been extensively applied in the *in vivo* investigation of many cardiovascular conditions [17], historically for research purposes [11, 13] and more recently as a viable clinical tool [17]. Although there is lack

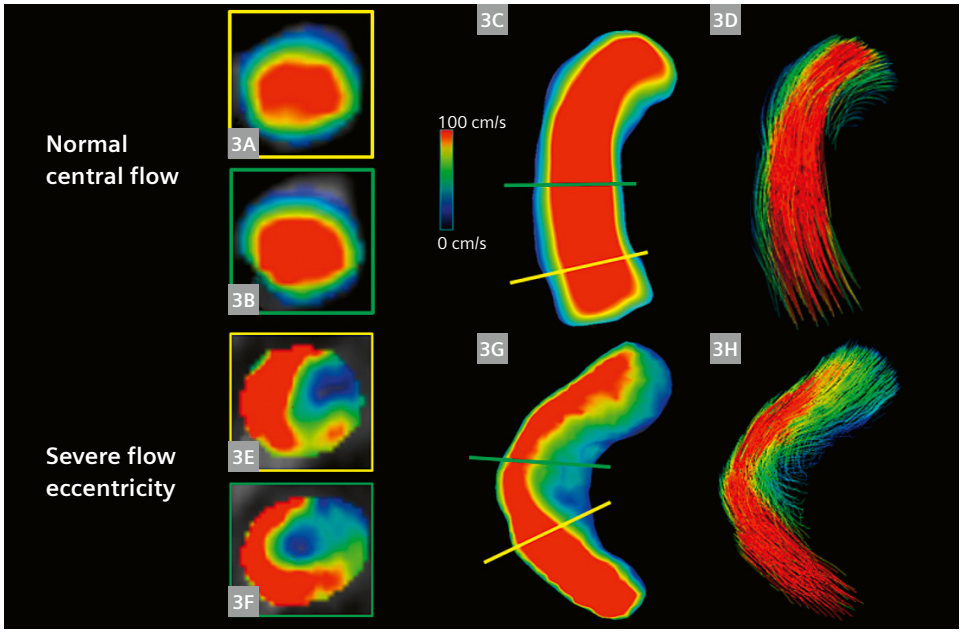

3 Flow eccentricity
Evaluation of flow eccentricity: Upper panels **(3A–3D)** show an example of velocity maps of normal central flow at the level of the sinotubular junction **(3A)** and the mid-ascending aorta **(3B)**; lower panels **(3E–3H)** show an example of velocity maps of a case with severe flow eccentricity at the level of the sinotubular junction **(3E)** and the mid-ascending aorta **(3F)**.

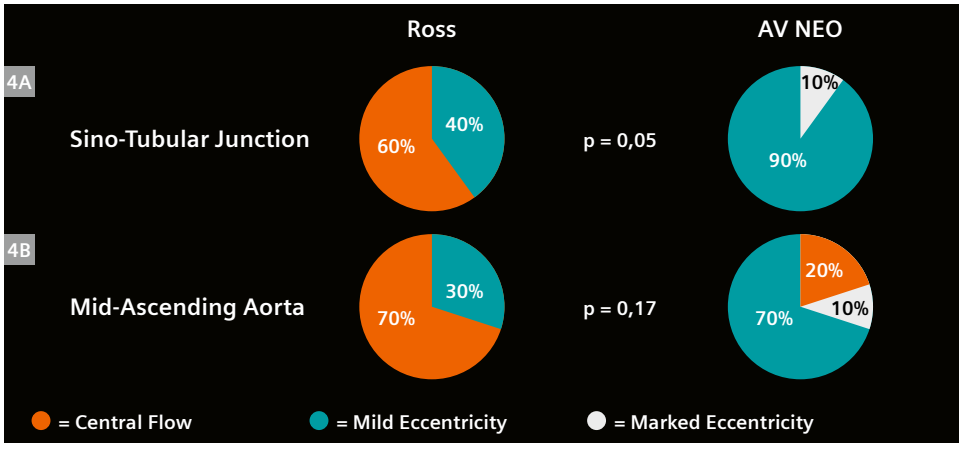

4 Flow patterns after Ross and AV Neo procedures: Results of flow evaluation at the level of the sinotubular junction **(4A)** and the mid-ascending aorta **(4B)** are shown, with no statistically significant differences found between the two groups.

of standardization, especially in children, several reports have provided WSS reference values for the thoracic aorta [21, 22]. In addition, hemodynamic consequences of aortopathies have been well investigated, even in children [19, 23].

In the current study, we measured and calculated *in vivo* cardiodynamic data in patients who underwent either the Ross or the AV Neo procedure.

Firstly, we recognized that average Vmax values were higher in the AV Neo group than in the Ross group, which was probably related to the smaller indexed aortic root diameters of AV Neo patients. The presence of flow acceleration in the early postoperative period after AV Neo has been previously described [8]. Interestingly, mid-term follow-up confirms that the natural excursion and "remodeling" of autologous cusps are distinctive features of the novel technique and that they can both contribute to a progressive and remarkable improvement of AV Neo hemodynamics compared to conventional AVR. Supporting this statement, blood flow distribution seemed to have a more prominent laminar flow at the sinotubular junction for AV Neo patients, with a p value close to statistical significance (p = 0.058).

Secondly, despite minor discrepancies among established determinants of theoretical WSS (velocity, vessel diameter, and flow eccentricity), both groups were comparable in terms of aortic WSS. In fact, no significant differences were observed in axial, circumferential, and global WSS measured at the sinotubular junction and at the mid-AAo. Although the main fluid-dynamic components differed between the two procedures when considered separately, overall WSS quantification by 4D Flow CMR showed similar hemodynamic performance. Notably, our results suggest that laminar flow and smaller vessel diameters probably balance the higher Vmax in the AV Neo group, while lower flow velocities seem to compensate for larger aortic roots and more prominent eccentric flow in the Ross group.

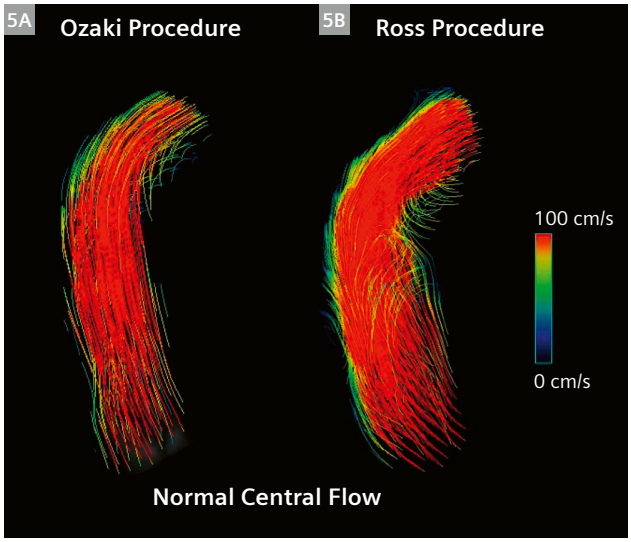

5 Comparison of ascending aortic 4D Flow profiles after the AV Neo procedure **(5A)** and the Ross procedure **(5B)**: Despite evidence of minor flow turbulences, both the Ozaki and the Ross procedure are equally able to restore fluid-dynamic conditions very close to normal physiology.

Conclusion

Nowadays, 4D Flow CMR has become a valuable tool for investigating fluid-dynamics in congenital and acquired cardiovascular disease such as aortic valvular disorders, providing new advanced features to assess blood-flow characteristics and their effects on the vessel wall.

The AV Neo procedure shows similar hemodynamic results to the Ross procedure in the short-term. Although slightly higher flow velocities are found in the AAo after AV Neo, both procedures are equally able to restore physiological tri-leaflet fluid-dynamic conditions. The AV Neo procedure generates similar short-term hemodynamic results in children needing AVR. The long-term durability of the technique remains to be proven.

		Ross (n = 10)	AV Neo (n = 10)	p
Sinotubular junction	WSS global$_{average}$ (N/m^2)	0.13 ± 0.05	0.16 ± 0.05	0.22
	WSS axial$_{average}$ (N/m^2)	0.14 ± 0.04	0.14 ± 0.07	0.93
	WSS circ$_{average}$ (N/m^2)	0.07 ± 0.03	0.07 ± 0.02	0.52
Mid-ascending aorta	WSS global$_{average}$ (N/m^2)	0.13 ± 0.05	0.14 ± 0.04	0.92
	WSS axial$_{average}$ (N/m^2)	0.13 ± 0.04	0.12 ± 0.02	0.36
	WSS circ$_{average}$ (N/m^2)	0.08 ± 0.02	0.08 ± 0.03	0.74

Table 3: **Wall shear stress (WSS) values according to the surgical procedure**
Values expressed as average and standard deviation;
*statistically significant p values ($p < 0.05$).

Acknowledgments

We would like to thank the 4D Flow "work in progress" sequence developers Daniel Giese and Jin Ning from Siemens Healthineers. We are also very thankful to the entire group of CMR radiographers and nurses collaborating in the CMR.

References

1 Akins CW, Miller DC, Turina MI, Kouchoukos NT, Blackstone EH, Grunkemeier GL, et al. Guidelines for reporting mortality and morbidity after cardiac valve interventions. Ann Thorac Surg. 2008;85(4):1490–1495.
2 Sharabiani MTA, Dorobantu DM, Mahani AS, Turner M, Peter Tometzki AJ, Angelini GD, et al. Aortic Valve Replacement and the Ross Operation in Children and Young Adults. J Am Coll Cardiol. 2016;67(24):2858–2870.
3 Ross DN. Replacement of aortic and mitral valves with a pulmonary autograft. Lancet. 1967;2(7523):956–958.
4 Elkins RC, Thompson DM, Lane MM, Elkins CC, Peyton MD. Ross operation: 16-year experience. J Thorac Cardiovasc Surg. 2008;136(3):623-30, 630.e1–5.
5 Takkenberg JJM, Kappetein AP, van Herwerden LA, Witsenburg M, van Osch-Gevers L, Bogers JJC. Pediatric autograft aortic root replacement: A prospective follow-up study. Ann Thorac Surg. 2005;80(5):1628–1633.
6 Etnel JRG, Elmont LC, Ertekin E, Mokhles MM, Heuvelman HJ, Roos-Hesselink JW, et al. Outcome after aortic valve replacement in children: A systematic review and meta-analysis. J Thorac Cardiovasc Surg. 2016;151(1):143–152.e1–3.
7 Ozaki S, Kawase I, Yamashita H, Uchida S, Nozawa Y, Matsuyama T, et al. Aortic valve reconstruction using self-developed aortic valve plasty system in aortic valve disease. Interact Cardiovasc Thorac Surg. 2011;12(4):550–553.
8 Ozaki S, Kawase I, Yamashita H, Uchida S, Takatoh M, Kiyohara N. Midterm outcomes after aortic valve neocuspidization with glutaraldehyde-treated autologous pericardium. J Thorac Cardiovasc Surg. 2018;155(6):2379–2387.
9 Wiggins LM, Mimic B, Issitt R, Ilic S, Bonello B, Marek J, et al. The utility of aortic valve leaflet reconstruction techniques in children and young adults. J Thorac Cardiovasc Surg. 2020;159(6):2369–2378.
10 Baird CW, Sefton B, Chávez M, Sleeper LA, Marx GR, Nido PJ del. Congenital aortic and truncal valve reconstruction utilizing the Ozaki technique: Short-term clinical results. J Thorac Cardiovasc Surg. 2020;S0022-5223(20)30438-4.
11 Bissell MM, Hess AT, Biasiolli L, Glaze SJ, Loudon M, Pitcher A, et al. Aortic dilation in bicuspid aortic valve disease: Flow pattern is a major contributor and differs with valve fusion type. Circ Cardiovasc Imaging. 2013;6(4):499–507.
12 Meierhofer C, Schneider EP, Lyko C, Hutter A, Martinoff S, Markl M, et al. Wall shear stress and flow patterns in the ascending aorta in patients with bicuspid aortic valves differ significantly from tricuspid aortic valves: a prospective study. Eur Heart J Cardiovasc Imaging. 2013;14(8):797–804.
13 Kelm M, Goubergrits L, Fernandes JF, Biocca L, Pongiglione G, Muthurangu V, et al. MRI as a tool for non-invasive vascular profiling: A pilot study in patients with aortic coarctation. Expert Rev Med Devices. 2016;13(1):103–12.
14 Guzzardi DG, Barker AJ, Ooij P Van, Malaisrie SC, Puthumana JJ, Belke DD, et al. Valve-Related Hemodynamics Mediate Human Bicuspid Aortopathy: Insights From Wall Shear Stress Mapping. J Am Coll Cardiol. 2015;66(8):892–900.
15 Bissell MM, Loudon M, Hess AT, Stoll V, Orchard E, Neubauer S, et al. Differential flow improvements after valve replacements in bicuspid aortic valve disease: a cardiovascular magnetic resonance assessment. J Cardiovasc Magn Reson. 2018;20(1):10.
16 Polito A, Albanese SB, Cetrano E, Cicenia M, Rinelli G, Adriano C. Aortic valve neocuspidalization in paediatric patients with isolated aortic valve disease: early experience. Interact Cardiovasc Thorac Surg. 2021;32(1):111–117.
17 Dyverfeldt P, Bissell M, Barker AJ, Bolger AF, Carlhäll C-J, Ebbers T, et al. 4D flow cardiovascular magnetic resonance consensus statement. J Cardiovasc Magn Reson. 2015;17(1):72.
18 Hope MD, Hope TA, Crook SES, Ordovas KG, Urbania TH, Alley MT, et al. 4D flow CMR in assessment of valve-related ascending aortic disease. JACC Cardiovasc. Imaging. 2011;4(7):781–787.
19 von Knobelsdorff-Brenkenhoff F, Trauzeddel RF, Barker AJ, Gruettner H, Markl M, Schulz-Menger J. Blood flow characteristics in the ascending aorta after aortic valve replacement – a pilot study using 4D-flow MRI. Int J Cardiol. 2014;170(3):426–433.
20 Chivers SC, Pavy C, Vaja R, Quarto C, Ghez O, Daubeney PEF. The Ozaki Procedure With CardioCel Patch for Children and Young Adults With Aortic Valve Disease: Preliminary Experience – a Word of Caution. World J Pediatr Congenit Heart Surg. 2019;10(6):724–730.
21 Davies PF. Hemodynamic shear stress and the endothelium in cardiovascular pathophysiology. Nat. Clin. Pract. Cardiovasc Med. 2009;6(1):16–26.
22 Callaghan FM, Grieve SM. Normal patterns of thoracic aortic wall shear stress measured using four-dimensional flow MRI in a large population. Am J Physiol Heart Circ Physiol. 2018;315(5):H1174–H1181.
23 Callaghan FM, Kozor R, Sherrah AG, Vallely M, Celermajer D, Figtree GA, et al. Use of multi-velocity encoding 4D flow MRI to improve quantification of flow patterns in the aorta. J Magn Reson Imaging. 2016;43(2):352–363.
24 Rose MJ, Rigsby CK, Berhane H, Bollache E, Jarvis K, Barker AJ, et al. 4-D flow MRI aortic 3-D hemodynamics and wall shear stress remain stable over short-term follow-up in pediatric and young adult patients with bicuspid aortic valve. Pediatr Radiol. 2019;49(1):57–67.

Contact

Aurelio Secinaro, M.D.
Bambino Gesù Children's Hospital IRCCS
Department of Imaging
Piazza S. Onofrio 4,
00165 Rome
Italy
Phone: + 39 06 68592792
Fax: + 39 06 68592394
aurelio.secinaro@opbg.net

Aurelio Secinaro

Paolo Ciancarella